International Journal of Engineering, Mathematical and Physical Sciences
ISSN: 2517-9934
Vol:8, No:2, 2014

A Boundary Fitted Nested Grid Model for Tsunami Computation along Penang Island in Peninsular Malaysia

Md. Fazlul Karim, Ahmad Izani Ismail, Mohammed Ashaque Meah

***Abstract*—**This paper focuses on the development of a 2-D boundary fitted and nested grid (BFNG) model to compute the tsunami propagation of Indonesian tsunami 2004 along the coastal region of Penang in Peninsular Malaysia.

In the presence of a curvilinear coastline, boundary fitted grids are suitable to represent the model boundaries accurately. On the other hand, when large gradient of velocity within a confined area is expected, the use of a nested grid system is appropriate to improve the numerical accuracy with the least grid numbers.

This paper constructs a shallow water nested and orthogonal boundary fitted grid model and presents computational results of the tsunami impact on the Penang coast due to the Indonesian tsunami of 2004. The results of the numerical simulations are compared with available data.

***Keywords*—**Boundary Fitted Nested Model, Tsunami, Penang Island, 2004 Indonesian Tsunami.

I. Introduction

IN the last couple of decades, a great deal of effort has been undertaken to incorporate irregular boundaries of coast and island to facilitate the computation of flow in various complicated region. For a numerical model using the curvilinear coordinate system, boundary fitted grids can be used to incorporate the space of the solution domain (e.g. the coastal waters of Peninsular Malaysia) in the physical space. This physical domain is then recorded onto a set of connected rectangular mesh with fixed grid spacing in the transformed computational domain, where the curvilinear coordinates serves as independent variables. Simulations are then carried out in the computational domain [2].

Finite difference technique representing the boundary as a stair step may give inaccurate results near the coastal area where computation results are of greatest interest and relevance for many studies. A boundary-fitted curvilinear grid system combines the ad vantages of finite-difference discretisation with grid flexibility. Boundary fitted grid makes the governing equations and boundary conditions simple and can better represent the geometry of the domain with a relatively lesser number of grid points. However, the gridline of the numerical scheme are curvilinear and non-orthogonal. Rectangular grid system is required to apply a regular finite difference scheme. In a boundary-fitted model, using appropriate transformations, the curvilinear boundaries are transformed into straight ones, so that in the transformed computational domain regular finite difference techniques can be used.

A considerable number of papers have been published on modelling the 2004 Indonesian tsunami for the west coast of Peninsular Malaysia [8], [9], [16], [17]. These models are based on the vertically integrated shallow water models and are discretised by the finite-difference scheme in Cartesian coordinate system and the shorelines are represented by stair-steps. In a stair step model the boundaries of the coast are approximated along the closest gridlines of the numerical scheme and so the numerical accuracy depends on the grid size. For the stair step models of Roy and Ismail [16], Roy et al. [17], [18] and Karim et al. [8]–[10], a very fine mesh was not used, and the representation of the coastal boundaries in those models were not very accurate. A boundary fitted model to simulate 2004 Indonesian tsunami along the west coast of Malaysia and southern Thailand was developed by Karim et al. [9]. In all these studies, it is assumed that the initial displacement of water surface is equal to the instant shift of the seabed and this is not entirely appropriate as an important factor for determining the initial size of a tsunami is the amount of vertical sea floor deformation over a short period of time [4].

Large velocity gradient occurs to the near shore where the ocean depth varies abruptly. It has been noted that propagation and inundation of tsunami is involve different processes due to greatly varying depths along its path. Applying numerical scheme in the same computational domain at an equal spacing grid may not be economical in simulation process. A common approach that can be adopted is to employ nested grids: nested grids with fine- mesh cover the areas of interest to coarse-mesh ones over larger areas. Available nested grid tsunami modeling codes, based on shallow water equations, include MOST (Method of Splitting Tsunami) by Titov and Gonzalez [19], Imamura and Gica (TUNAMI-N2) [5], and Karim et al. [11], [12].

The west coast of Peninsular Malaysia is irregular in nature and there are many offshore islands. In order to get better estimation of water levels due to tsunami along the coast, incorporation of the boundaries of coast and island properly in a numerical scheme is important. Moreover, the south part of Malacca strait extended up to offshore of Penang is shallow

Md. F. Karim is with the Institut Teknologi Brunei, Brunei (phone: +673 7157167; e-mail: mdfazlulkk@yahoo.com).

A. I. Md. Ismail is with the Universiti Sains Malaysia, Malaysia (e-mail: izani@cs.usm.my).

M. A. Meah is with the Shahjalal University of Science and Technology, Bangladesh Institute Technology Brunei, Brunei (e-mail: mamsust@yahoo.com).

where the ocean depth is less than 50m [3]. On the other hand, the whole computational domain of the study (2º-14º N and 90º-100º30´E) includes eastern part of the Indian Ocean and the ocean depth in the deep sea is approximately 3500 m [12]. Since the wave velocity depends on the depth of the sea, and shallow water and deep sea regions exist in the model area, large velocity differences are expected near the boundary of the shallow regions.

In this study, in the light of the ocean depth near the shore and the irregular nature of Penang Island, a boundary-fitted and nested grid (BFNG) model is constructed and applied to compute the tsunami impact along the coastal regions of Penang Island in Peninsular Malaysia. Both methods are applied simultaneously within the same model. This study also takes the account the dynamics of sea bed deformation over a short period of time as an initial condition of tsunami generation which is more realistic.

Fig. 1 Model domain including west coast of Thailand, Peninsular Malaysia and west of North Sumatra covering the source zone

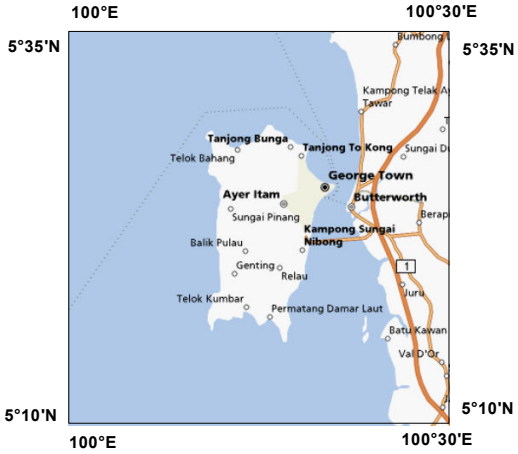

Fig. 2 Inner model domain includes Penang Island

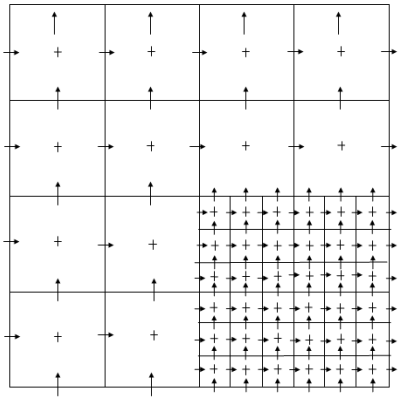

Fig. 3 Nested grids in inner model

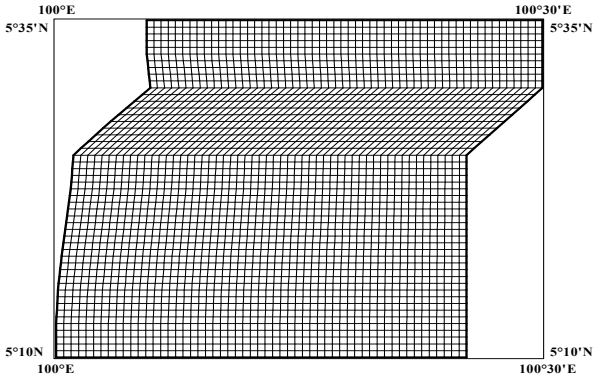

Fig. 4 Inner physical domain

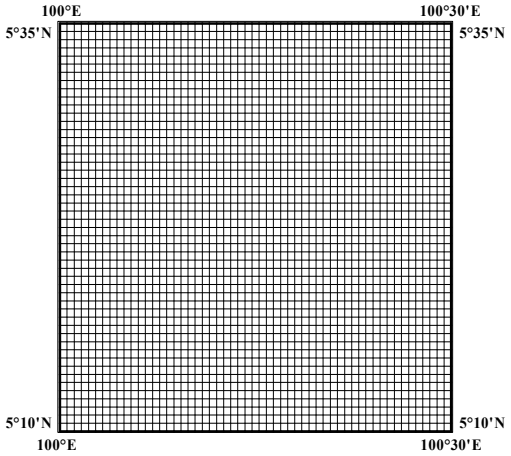

Fig. 5 Inner computational domain

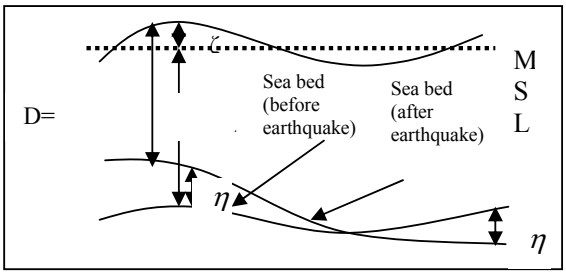

Fig. 6 Schematic diagram that shows the seabed deformation (η) and sea surface elevation (ς) from the mean sea level (MSL)

II. Numerical Model

Boundary-fitted curvilinear grid system is used since the boundaries of coast and islands are curvilinear in nature. By applying this method, the boundaries of both regions can be matched accurately. Then, necessary transformation is used to transform the curvilinear physical domain into a rectangular computational domain so that the proposed finite difference scheme can be applied to the system. In addition, the one-way nested grid approach is applied near the shore of Penang in order to increase the numerical accuracy. This means that an inner domain representing the regions of Penang is developed inside the outer domain (whole model domain) that covers the open sea that contains the epicenter of 2004 Sumatra-Andaman Earthquake together with coastal regions of Penang. Nested numerical approach is applied because the whole domain of computation consists of the open sea that covers the deep water and shallow water. Due to this fact, a large gradient of water velocities and sea surface elevations are expected near the coasts of both regions. In nested grid approach, grid size of inner domain is taken to be smaller compared to the grid size of outer domain so that results with greater accuracy can be obtained.

A. Depth Averaged Shallow Water Equations

To study tsunami events due to sea floor deformation (uplift and subsidence), the equations of continuity and motion are formulated in Cartesian coordinates and the established depth averaged equations of continuity and motions are

$$\frac{\partial \zeta}{\partial t} - \frac{\partial \eta}{\partial t} + \frac{\partial}{\partial x}[D\,u] + \frac{\partial}{\partial y}[D\,v] = 0 \qquad (1)$$

$$\frac{\partial u}{\partial t} + u\frac{\partial u}{\partial x} + v\frac{\partial u}{\partial y} - f\,v = -g\frac{\partial \zeta}{\partial x} - \frac{F_x}{\rho\, D} \qquad (2)$$

$$\frac{\partial v}{\partial t} + u\frac{\partial v}{\partial x} + v\frac{\partial v}{\partial y} + f\,u = -g\frac{\partial \zeta}{\partial y} - \frac{F_y}{\rho\, D}. \qquad (3)$$

In the above equations, u and v denotes the velocities in x and y directions, $m\ s^{-1}$, ς is the sea level, η is the sea bed displacement (Fig. 6), g is the acceleration of the earth gravity, and $D = h + \varsigma - \eta$ is the total depth of the sea. The Coriolis parameter is taken as $f = 2\Omega \sin\phi$, φ is the latitude of a location in the analysis area.

The bottom friction forces are:

$$\left.\begin{aligned} F_x &= \rho\, C_f\, u \left(u^2 + v^2\right)^{1/2} \\ F_y &= \rho\, C_f\, v \left(u^2 + v^2\right)^{1/2} \end{aligned}\right\} \qquad (4)$$

where, C_f is the friction coefficient and $\rho$is the water density, $kg\ m^{-3}$.

B. Model Data Set Up

The BFNG model domain is divided into two parts outer and inner domain. The outer physical domain of BFNG model with grid size 4km covers the whole model area (91°E to 100.5°E latitude and 2°N to 14°N longitude, Fig. 1 starting from the open sea up to the coastal belts of Penang Island in Peninsular Malaysia. The epicenter of the 2004 Indian Ocean Tsunami in Sumatra lies in this domain.

The computation is done at every 10 seconds, satisfying the finite difference stability condition. The friction coefficient value is taken as 0.0033 [13] throughout the model area. The ocean depth is taken from the Admiralty bathymetric charts.

In the numerical scheme the coastal and island boundaries are approximated by continuous segments either along the nearest y-directed odd gridline or along the closest x-directed even grid line. Thus each boundary is represented by a stair step. At each segment there exists only one velocity component normal to the segment. This will guarantee the zero normal velocity components at the boundary segment. Similar to Karim et al. [9], the origin of the Cartesian coordinate system is at O (3.125° E, 101.5° N), x-axis is directed towards west at an angle 15° with the latitude line through O and the y-axis is directed towards north inclined at an angle 15° with the longitude line through O.

C. Boundary Fitted Curvilinear Grid and Coordinate Transformation for Outer and Inner Scheme

Similar to Karim et al. [9], the coastal boundary on the east of the outer physical domain is presented by the function $x = b_1(y)$ while the western open sea boundary of the outer physical domain is defined by the function $x = b_2(y)$. The north and south open sea boundaries are set to be at $y = L$ and $y = 0$ respectively.

Similar to the outer model the eastern coastal boundary of the inner model (Fig. 2) is represented by $x = b_1(y)$ which is a part of the eastern coastal boundary of the outer model and situated at the same computational grid line. The western open sea boundary of the inner model is represented by $x = b_2(y)$ which is identical with a particular grid line of the outer model parallel to the *y*-axis. The north and south open-sea boundaries are situated at two particular grid lines of the outer model parallel to *x*-axis. The curvilinear grid lines parallel to *x*-axis and *y*-axis in the inner model are generated by the two generalized functions same as the outer model.

Similar coordinate transformation of Johns et al. [7] is used in treating the curvilinear boundary configuration to rectangular one. The physical and transformed computational domains and their grids of inner model are shown in Figs. 4 and 5 respectively.

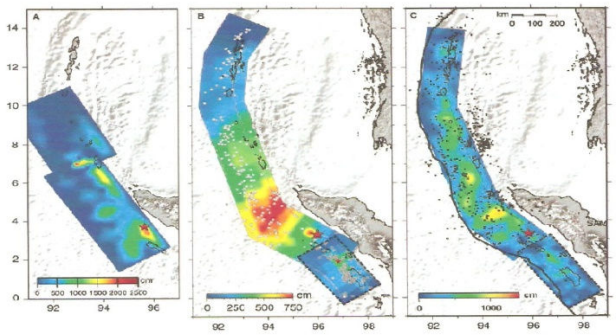

Fig. 7 Finite source slip models for the 2004 Sumatra-Andaman Earthquake (Source: Ammon et al. [1])

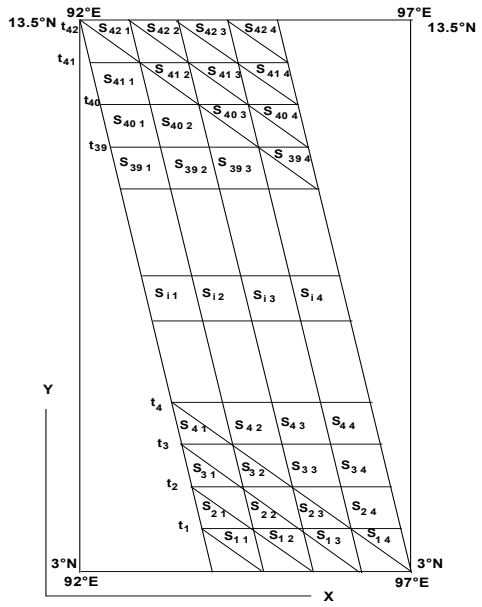

Fig. 8 Tsunami source activated into several segments over a short period of time

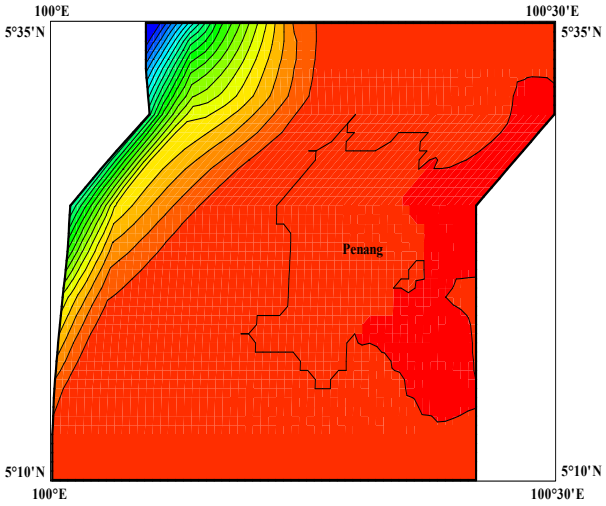

Fig. 9 Elevation of Tsunami propagation towards Penang Island at 200 minutes

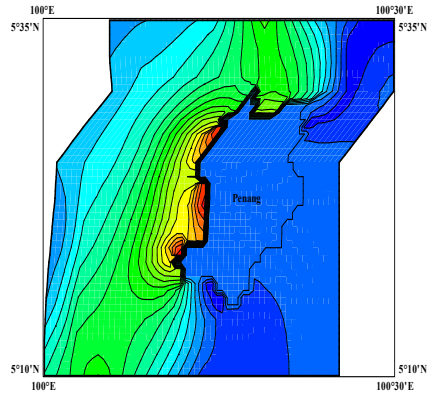

Fig. 10 Elevation of Tsunami propagation towards Penang Island at 240 minutes

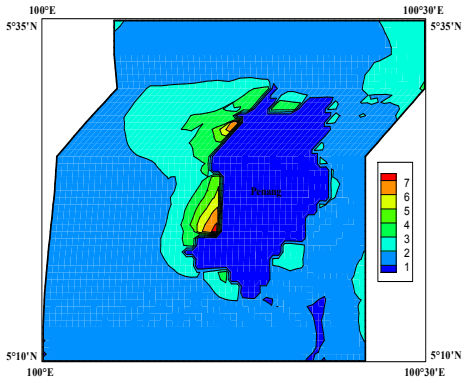

Fig. 11 Maximum water level computed around Penang Island in Peninsular Malaysia

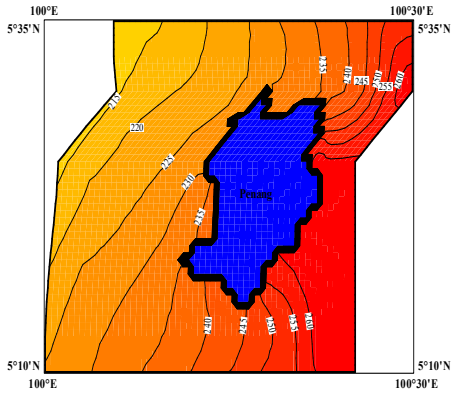

Fig. 12 Tsunami arrival time towards Penang Island

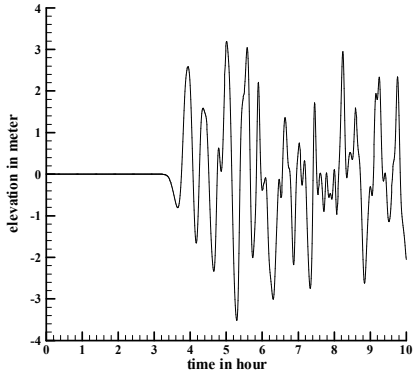

Fig. 13 (a) Water level computed at the north coastal positions in Penang Island associated with 2004 Indian Ocean Tsunami

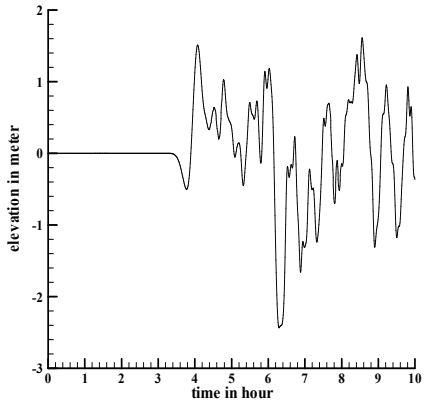

Fig. 13 (b) Water level computed at the north-west coastal positions in Penang Island associated with 2004 Indian Ocean Tsunami

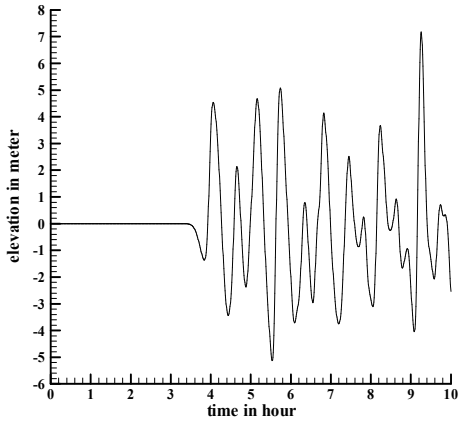

Fig. 13 (c) Water level computed at the south-west coastal positions in Penang Island associated with 2004 Indian Ocean Tsunami

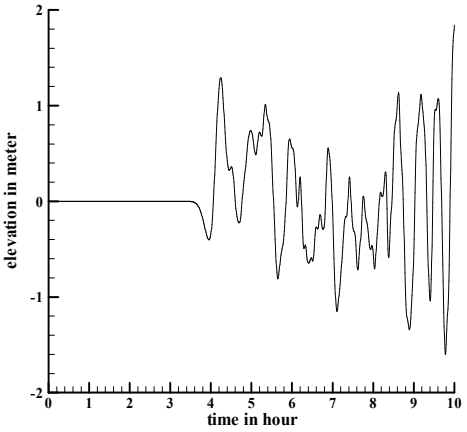

Fig. 13 (d) Water level computed at the south-east coastal positions in Penang Island associated with 2004 Indian Ocean Tsunami

D. Boundary Conditions of Outer and Inner Models

Similar to Karim et al. [9] the radiation boundary conditions for the north, south and west open sea boundaries of outer model are applied in this study to allow disturbance generated within the model area, to go out through the open boundary [7]. At the coastal belts of the main land and islands, the normal components of velocities are taken as zero (i.e. closed boundaries).

The outer model domain (2° N -14°N and 91°E -100.5°E) and the inner model domain ($5^{\circ}10'N$ - $5^{\circ}35'N$ and $100^{\circ}E$ - $100^{\circ}30'E$) are shown in Figs. 1 and 2 respectively. The outer and inner domains are discretised with square grids of sizes 4 km and 0.8 km respectively. Computational results of outer model (u, v, ς) are interpolated and then used as input into inner nested model domain as initial conditions.

The coupling of the coarser and finer schemes is done according to Johns et al. [7], who maintained the one way interaction between the parent (outer) and nested schemes (Fig. 3) of the inner model.

III. Initial Condition (Tsunami Source and Its Implementation in Outer Model)

Several investigations have been devoted for determining rupture zone associated with the event of 2004 [15], [1], [6], [14]. All the above mentioned studies suggest that the distribution of aftershocks and seafloor deformations indicate a time progression of the rupture with 3 – 4 separate subzones (Fig. 7) and the rupture length is approximately 1200 to 1300 km. Thus, the initial disturbance of the sea surface along the source zone is time dependent. The extent of rupture between 93–97°E and 3–11°N of the seabed was reported in Kowalik et al. [13]. The tsunami source is extended along the fault zone from south-east to north-west.

Our present study takes into account the dynamics of seabed displacement over a short period and do not consider the waveform as instantly generated.

Based on rupture parameters estimated by several authors, a reasonable tsunami source has been constructed for the event 26 December of 2004 in terms of magnitude and timing of seabed displacement. A rectangular source extended along the fault line (92–97°E and 2–13.5°N) having length ~ 1200km and width ~ 300km is considered in this study. This rectangular zone has been divided into 42×4 segments as shown in Fig. 8. We designate the segments by S_{ij} where i = 1, 2,…,42; j = 1, 2, 3, 4. Starting from S_{11} at the southwest corner of the rectangular source zone we activate the whole source in 45 time steps (in 450 seconds) in the way, shown in Table I.

TABLE I
Tsunami Source Activations

Time Step	Segment Activated
1	S_{11}
2	S_{21} S_{12}
3	S_{31} S_{22} S_{13}
4	S_{41} S_{32} S_{23} S_{14}
.	.....
.	.....
.	.....
k	S_{k1} $S_{k-1\ 2}$ $S_{k-2\ 3}$ $S_{k-3\ 4}$
k=4, 5,…..,42	
.	.....
.	.....
.	.....
42	$S_{42\ 1}$ $S_{41\ 2}$ $S_{40\ 3}$ $S_{39\ 4}$
43	$S_{42\ 2}$ $S_{41\ 3}$ $S_{40\ 4}$
44	$S_{42\ 3}$ $S_{41\ 4}$
45	$S_{42\ 4}$

Thus the source has been activated gradually from south to north and from west to east as shown in Fig. 8. Based on the information outlined in this section, we consider the source with maximum rise of 5m and maximum fall of 4.75 m of the seabed from west to east. In our model simulation, the magnitude of sea bed deformation in different segments of rupture zone is taken from the source deformation contours, Fig. 4 of Kowalik et al. [13]. The initial sea floor displacement and the velocity components are taken as zero everywhere.

IV. Results and Discussions

A. Results Obtained from Boundary-Fitted Inner Nested Scheme

The equations (1)-(3) along with the boundary conditions of the BFNG model are solved by using the finite difference method. Tsunami wave field in a Cartesian coordinates is computed and wave heights along the coastal belts of Penang Island are estimated.

B. Tsunami Propagation Using BFNG Model

Model simulations using the source outlined in Section III were made for 10 hours of propagations. Tsunami propagation in the form of contour at two different instants of time is presented in Figs. 9 and 10. In this simulation using the BFNG model, 0.1m sea level enhancement is considered as the arrival of tsunami. It is observed that after initiating the source, the tsunami wave propagated around the Indian Ocean and arrived at the Shore of Penang Island at 200 minutes (Fig. 9). Then it gradually proceeds towards the east, surrounding the island and reaches the east coast 40 minutes later (Fig. 10).

C. Maximum Water Level around Penang Island Using BFNG Model

During this computation the maximum enhancement of the sea level is recorded. Maximum sea surface level in the form of contours along the Coast of Penang Island is shown in Fig. 11. This figure shows that the surge amplitude is increasing along the coast from south to north. The maximum tsunami height of 2.5 – 7m was observed at Penang Island. The tsunami height is increasing very fast near the shoreline everywhere. Both observation and computation demonstrate the similar trend along Penang. The computed water levels using the BFNG model indicate that the north and west coasts of Penang Island is vulnerable for stronger surges.

D. Arrival Time of Tsunami Using BFNG Model

Correct computation of arrival time, could be important for evacuation planning. Fig. 12 shows the arrival time of tsunami towards Penang Island using the BFNG model. It is seen that tsunami continue to propagate towards Penang Island in Peninsular Malaysia after its initiation at Sumatra. The first wave was found to hit the North-West Coast of Penang Island at 230 minutes after the initial tsunami generation at the source. Then, the tsunami waves continue propagating towards the south west coast of Penang and after 10 minutes it "flooded" the north-west coast of the island. At 245 minutes after the initial tsunami generation, the south coast of Penang was flooded by the waves. The tsunami waves continue proceeding and surrounding the island and finally at 260 minutes, almost the whole coastal areas of Penang Island was "flooded" by the tsunami.

The USGS website [(http://staff.aist.go.jp/kenji.satake/Sumatra-E.html) (Tsunami travel time in hours for the entire Indian Ocean)] confirms the fact that the arrival time of tsunami at Penang is between 4 hr and 4 hr 30 min. Hence the observe arrival time available in USGS closely matches the calculated tsunami arrival time using the BFNG model.

D. Computed Time Series of Water Levels along the Penang Island Using BFNG Model

The record of calculated water levels at different locations of the coastal belt of Penang Island had a sampling interval of 30 secs. Fig. 13 depicts the time series of water levels at four locations on the north, north-west, south and south-east coasts of Penang Island. At Batu Ferringhi (north coast), the first train of wave arrived at this site, 4 hr after the shock. The maximum enhancement in this train was 2.4m (Fig. 13 (a)). At approximately 4hr 20min after the shock, the second wave train arrived with tsunami height of 1.4m. Then, at approximately, 5hr after the shock, the third and the highest wave train arrived, with a maximum height of 3.1m. The water level oscillates for several hours. Gaze records of tsunami also show the same pattern; for example deep ocean bottom pressure recorder records, of water level at different locations in the Pacific Ocean during the 1996 Andreanov earthquake, show that oscillation continues for long time (see Fig. 3 of [19]). At the location Pantai Aceh (north-west) the maximum elevation is approximately 1.8 m (Fig. 13 (b)). Near Pasir Panjang (south-west) the maximum elevation of the first wave train is found to be 4.1m (Fig. 13 (c)). At the south-east coast the calculated maximum surge level is found to be 1.4m (Fig. 13 (d)). The calculated Tsunami record at different locations of Penang Island using the BFNG model is similar to the field measurement [16].

The results obtained for maximum water level, travel time and time series of sea surface elevation using the BFNG model are just slightly quantitatively different from those obtained in our previous studies [10] on the impact of 2004 tsunami on Penang Island.

V. Conclusion

In this study, a BFNG model is developed and the model is applied for tsunami computation of 2004 Indonesian tsunami along the coastal belts of Penang Island. In the BFNG model, it has been possible to transfer reasonable values for the open boundaries of the inner scheme from the outer. It is found that BFNG model results give satisfactory agreement with available data and previous computations.

Acknowledgment

This research is supported by the research grant by the Government of Brunei and the authors acknowledge the support.

References

[1] Ammon, J.C., Ji, C., Thio, H., Robinson, D., Ni, S., Hjorleifsdottir, V., Kanamori, H., Lay, T., Das, S., Helmberger, D., Ichionose, G., Polet, J. and Wald, D., "Rupture Process of the 2004 Sumatra-Andaman Earthquake" Science 308, 1133-1139, 2005.

[2] Chan, C. T., Cheong, H. F., and Shankar, N. J., "A boundary-fitted grid model for tidal motions: Orthogonal coordinates generation in 2-D embodying Singapore coastal waters", Journal of Computers Fluids, 23 (7), 881-893, 1994.

[3] Dao, M. H., and Tkalich, P., "Tsunami propagation modeling-a sensitivity study", Natural hazards and earth system sciences, 7, 741 – 754, 2007.

[4] Iguchi, T., "A mathematical analysis of tsunami generation in shallow water due to sea bed deformation", Proceedings of the Royal Society of Edinburgh, 141A, 551-608, 2011.

[5] Imamura, F., and Gica, E. C., "Numerical Model for Tsunami Generation due to Subaqueous Landslide Along a Coast –A case study of the 1992 Flores tsunami, Indonesia", Sc. Tsunami Hazards, 14(1),13 – 28, 1996.

[6] Ishii, M., Shearer, P. M., Houston, H., and Vidale, J.H., "Extent, duration and speed of the 2004 Sumatra-Andaman earthquake imaged by the Hi-Net array" Nature 435(7044), 933-936, 2005.

[7] Johns, B., Rao, A. D., Dube, S. K., and Sinha, P. C., "Numerical modelling of tide-surge interaction in the Bay of Bengal", Phil. Trans. Roy. Soc. London A 313, 507 – 535, 1985.

[8] Karim, M. F., Roy, G. D., Ismail, A. I. M., and Meah, M. A., "A linear Cartesian coordinate shallow water model for tsunami computation along the west coast of Thailand and Malaysia" Int. J. of Ecology & Development" 4(S06): 1 – 14, 2006.

[9] Karim, M. F., Roy, G. D., Ismail, A. I. M., and Meah, M. A., "A shallow water model for computing tsunami along the west coast of Peninsular Malaysia and Thailand using boundary-fitted curvilinear grids" Journal of Science of Tsunami Hazards, 26 (1), 21 – 41, 2007a.

[10] Karim, M. F., Roy, G. D., and Ismail, A. I. M., "An Investigation on the Effect of Different Orientation of a Tsunami Source along the Coastal Belt of Penang Island: A Case Study of the Indonesian Tsunami 2004" Far East J. of Ocean Research, 1 (1), 2007, 33-47, 2007b.

[11] Karim, M. F., Roy, G. D., Ismail, A. I. M.; and Meah, M.A., "Numerical Simulation of Indonesian Tsunami 2004 along Southern Thailand: A

Nested Grid Model", International Journal of Mathematical, Physical and Engineering Sciences, volume 3 (1), 8-14, 2009a.

[12] Karim, M. F., Ismail, A. I. M.; and Meah, M.A., "Numerical Simulation of Indonesian Tsunami 2004 at Penang Island in Peninsular Malaysia using a Nested Grid Model, International Journal of Mathematical Models and Methods in Applied Sciences, Issue 1, volume 3, 1-8, 2009b".

[13] Kowalik, Z., Knight, W., and Whitmore, P. M., "Numerical Modeling of the Global Tsunami: Indonesian Tsunami of 26 December 2004" J. of Sc. Tsunami Hazards. 23(1), 40 – 56, 2005.

[14] Lay, T., Kanamori, H., Ammon, J. C., Nettles, M., Steven., N. W., Aster, R., Susan, L. B., Michael, R., B., and Butler, B., " The great Sumatra-Andaman Earthquake of 26 December 2004" Science 308, 1127-1133, 2005.

[15] Ni, S., Kanamori, H., and Helmberger, D., "Energy radiation from the Sumatra Earthquake" Nature 434(7033), 582-582, 2005.

[16] Roy, G. D., and Ismail, A. I. M., "An investigation on the propagation of 26 December 2004 tsunami waves towards the west coast of Malaysia and Thailand using a Cartesian coordinates shallow water model" Proceedings of international conference in Mathematics and Applications, Mahidol University, Thailand 389-410, 2005.

[17] Roy, G. D., Karim, M. F., and Ismail, A. M., " Numerical Computation of Some Aspects of 26 December 2004 Tsunami along the West Coast of Thailand and Peninsular Malaysia Using a Cartesian Coordinate Shallow Water Model", Far East J. of Applied Mathematics, 25(1), 57-71, 2006.

[18] Roy, G. D., Karim, M. F., and Ismail, A. M., "A Non-Linear Polar Coordinate Shallow Water Model for Tsunami Computation along North Sumatra and Penang Island" Continental Shelf Research, 27, 245–257, 2007.

[19] Titov, V. V., and Gonzalez, F. I., "Implementation and Testing of the Method of Splitting Tsunami (MOST) Model" NOAA Technical Memorandum ERL, PMEL – 112, Contribution No. 1927 from NOAA/Pacific Marine Environmental Laboratory, pp 11, 1997.